Tailoring the Magneto-Optical Properties of Vanadate Sodium Tellurite Glasses via Zinc Doping for Device Applications

Yamagouni Paramesh Goud[1], Nirlakalla Ravi[2,*] Renigunta Padmasuvarna[1]

[1]Department of Physics, Jawaharlal Nehru Technological University Anantapur, Anantapuramu, India-515002.
[2]Glass-Ceramics Lab, Department of Physics, Rajeev Gandhi Memorial College of Engineering and Technology, Nandyal, India-518501.

Abstract

Tellurite glasses doped with V_2O_5, Fe_2O_3, Na_2O, and ZnO (TVFNZn) have been extensively studied for their structural, magnetic, and optical properties. Analysis using Fourier transform infrared (FTIR) and micro-Raman spectroscopy identified characteristic bands at 470, 660, 695, 808, 905, 955, 1648, 2348, 2890, and 3417 cm^{-1}. The band observed at 695 cm^{-1} is attributed to the stretching vibrations of Te-O bonds in TeO_3^{+1} or TeO_3 units. Raman spectroscopy further revealed bands at 127, 290, 469, 672, 732, 872, and 935 cm^{-1}, with the band at 672 cm^{-1} corresponding to the asymmetric stretching vibration of Te-O bonds in the $[TeO_4]^{4-}$ bipyramidal structure. Electron spin resonance analysis detected a signal at a magnetic field strength of 45.83 mT with a g-factor of 2.09. Magnetic hysteresis measurements using a vibrating sample magnetometer showed a coercivity of 2.2622 mT, a remanence of 22.883 × 10^{-3} Am^2/kg, and a saturation magnetization of 0.2799 Am^2/kg. In the optical absorption spectrum, an ultraviolet band at 346 nm is associated with TeO_2, while absorption bands typical of V_2O_5 are observed in the 200–300 nm range.These results highlight the potential of TVFNZn glasses for use in magneto-optical applications, showcasing their promising structural, magnetic, and optical characteristics.

Keywords: Tellurite glasses, ZnO, structural, magnetic, optical properties

1 Introduction

Magneto-optical (MO) materials have gained considerable attention due to their wide-ranging applications in optical switches, isolators, circulators, modulators, secure encoding, and sensing technologies. Among these, optical isolators and circulators are particularly critical in optical systems, as they either ensure unidirectional light propagation or shield upstream components from the effects of backward-propagating light [1,2]. MO glasses leverage the Faraday effect, which involves the rotation of the polarization plane of light when subjected to a magnetic field along the direction of propagation. Enhancing the Faraday effect in glasses requires incorporating a high concentration of paramagnetic elements, such as rare earth (RE^{3+}) ions and certain transition metal oxides [TMOs] [3]. This effect arises from circular anisotropy in the magnetized medium, which is a result of the longitudinal Zeeman effect—splitting of the ground and excited states in the presence of a magnetic field [4]. The ongoing advancement of magneto-optical devices necessitates the development of innovative glass materials with high Verdet constants and low absorption properties [5].

Tellurite glasses are highly regarded for their potential in both linear and nonlinear optical applications. These glasses exhibit several advantageous properties, including low phonon energy, a high refractive index, a low melting point, strong chemical resistance, thermochromic behavior, good mechanical strength, a high dielectric constant, and excellent transparency across the visible and infrared (IR) spectrum.Tellurium dioxide (TeO_2), a conditional glass former, requires rapid cooling to form a glassy state. It is also an excellent host material for rare-earth-doped glasses because its weak Te–O bonds can easily break, allowing heavy metal and rare earth atoms to integrate into the glass network [6-10]. Notably, tellurite glasses demonstrate extended transmission in the infrared region. Their ease of fiber drawing at low temperatures and high capacity to dissolve rare earth ions make them valuable for use in optical components for sensors, telecommunications, and medical applications [11].

Furthermore, studies suggest that the presence of non-bridging oxygen leads to structural transformations within the glass network, where TeO_4 trigonal bipyramids (tbp) convert into TeO_3 trigonal pyramids (tp). This structural flexibility contributes to the unique properties of tellurite glasses [12].

Numerous studies have emphasized the impact of incorporating transition metals like V_2O_5 into glass, highlighting its role in enhancing the semiconducting properties of the material. Changes in thermal and optical properties due to such additions have also been extensively investigated [13-17]. Vanadium exhibits multiple oxidation states, with trivalent (V^{3+}), tetravalent (V^{4+}, also known as vanadyl), and pentavalent (V^{5+}, also referred to as vanadate) being the most notable, with V^{4+} and V^{5+} being the most prevalent. Vanadium pentoxide (V_2O_5) is a strong oxidizing agent with a wide range of applications. These include industrial uses, such as in batteries and solar cells, as well as biological applications, such as biosensors for detecting macromolecules, and pharmacological uses [18-20]. Glasses doped with transition metal oxides like V_2O_5 are recognized for their semiconducting properties, making them suitable for various advanced technological and scientific applications.

Research on binary Fe_2O_3–TeO_2 glasses prepared via melt quenching remains limited, with some studies reporting IR spectroscopy and magnetization data for samples where x = 0.1 to 0.30 [21, 22]. Magnetization measurements indicate that these samples exhibit paramagnetic behavior due to the presence of Fe_2O_3. Glasses composed of a combination of transition metal oxides (TMOs) such as V_2O_5, Fe_2O_3, and ZnO, along with alkali metals like Na_2O, are known to exhibit mixed ionic and electronic conductivity. In recent years, the exploration of such mixed electronic–ionic conductors has expanded significantly, driven by their potential applications in advanced technologies, including cathodes for electrochemical cells and smart windows.

This research paper proposes various TMOs with magnetic properties and alkali metal oxides (Na2O) doped tellurite glasses were explored for structural, magnetic and optical properties for magneto-optical device applications.

2 Experimental work

A 10 g batch of glass from equation (1) was prepared using high-purity powders measured in precise stoichiometric ratios according to the specified formula. The powders were thoroughly ground for one hour using an agate mortar and pestle to ensure homogeneity in the mixture. The homogenized mixture was then transferred to a high-purity alumina crucible and placed in a programmable furnace. The mixture was melted at 1150°C in an air atmosphere for 2 hours.After melting, the molten material was rapidly extracted from the furnace and air-quenched by pouring it onto a preheated brass plate at room temperature. The resulting glass was then annealed in a furnace at 350°C for 16 hours to relieve internal stresses and eliminate air bubbles. The glass was gradually cooled to room temperature before being sliced into small pieces. These samples were subsequently powdered and prepared for further characterization to analyze their various properties.

$$40\ TeO_2 + 25\ V_2O_5 + 20\ Na_2O + 10\ Fe_2O_3 + 5ZnO\ (TVFNZn) \quad (1)$$

3 Characterization techniques

The FTIR spectra of the TVFN glass were recorded using a Perkin Elmer Spectrum Two spectrometer in the range of 4000–400 cm^{-1}. Micro-Raman analysis was performed with a Horiba Jobin Yvon LabRAM HR spectrometer, operating in the range of 50–3000 nm. Electron spin resonance (ESR) measurements were conducted using a JEOL JES-FA200 spectrometer (Japan) equipped with X and Q bands, featuring a sensitivity of 7×1097 \times 10^9 spins/0.1 mT and a resolution of 2.35 μT. The magnetic properties of the TVFN glasses were analyzed using a Lakeshore vibrating sample magnetometer (VSM), model 7410 series, with a maximum applied field of 31 kOe (3.1 T), a field resolution of 0.1 Oe at 35 kOe, and a

temperature range of 100 K to 1273 K. The field accuracy was specified as 1% of the reading or 0.05% of the full scale (0.1×10^{-6} to 1000 Am^2/kg). Additionally, absorption spectra in the range of 0–2500 nm were measured using a Varian CARY 5000 spectrophotometer equipped with a tungsten lamp.

4 Results and discussion

4.1FT-IR analysis

The Fourier transform infrared (FT-IR) transmittance spectra shown in Fig. 1(a) at room temperature revealed the presence of TVFNZn glass's structural groups in the waveneumber range of 4000 to 400 cm^{-1}. Absorption bands at wavenumbers 470, 660, 695, 808, 905, 955, 1648, 2348, 2890, and 3417 cm^{-1} are seen in the TVFNZn glasses. The tiny bands seen at 470 cm^{-1} are caused by vibrations caused by the Zn-O bond stretching in TVFNZn glasses [23, 24]. The symmetric stretching mode of Te-O-Te vibrations is represented by the band at 491 cm^{-1}. The Te-O stretching vibrations in the TeO_4 trigonal bipyramid seen in Fig. 1(b) are shown by a band at 660 cm^{-1}. The stretching vibration of Te-O bonds in TeO_{3+1} or TeO_3 units is specified by an additional band at 695 cm^{-1} [25, 26]. The distinctive spectral bands seen in V_2O_5 at 955 and 905 cm^{-1} are associated with the symmetrical stretching vibration of terminal oxygen bonds, V=O (905 cm^{-1}), and the vibrations of doubly coordinated oxygen (bridge oxygen) bonds, V–O–V (955 cm^{-1}), respectively [27]. At 1648 cm^{-1}, a little band caused by H-O-H bending of absorbed water or Fe-O-Te stretching vibrations was seen [28]. Furthermore, the vibrations of the OH-molecule in the glass are represented by the bands 2890, 2348 and 3417 cm^{-1}. The biggest absorption peak was detected at 695 cm^{-1}, indicating that the TVFNZn glasses are important in the luminosity characteristic and have a low phonon energy.

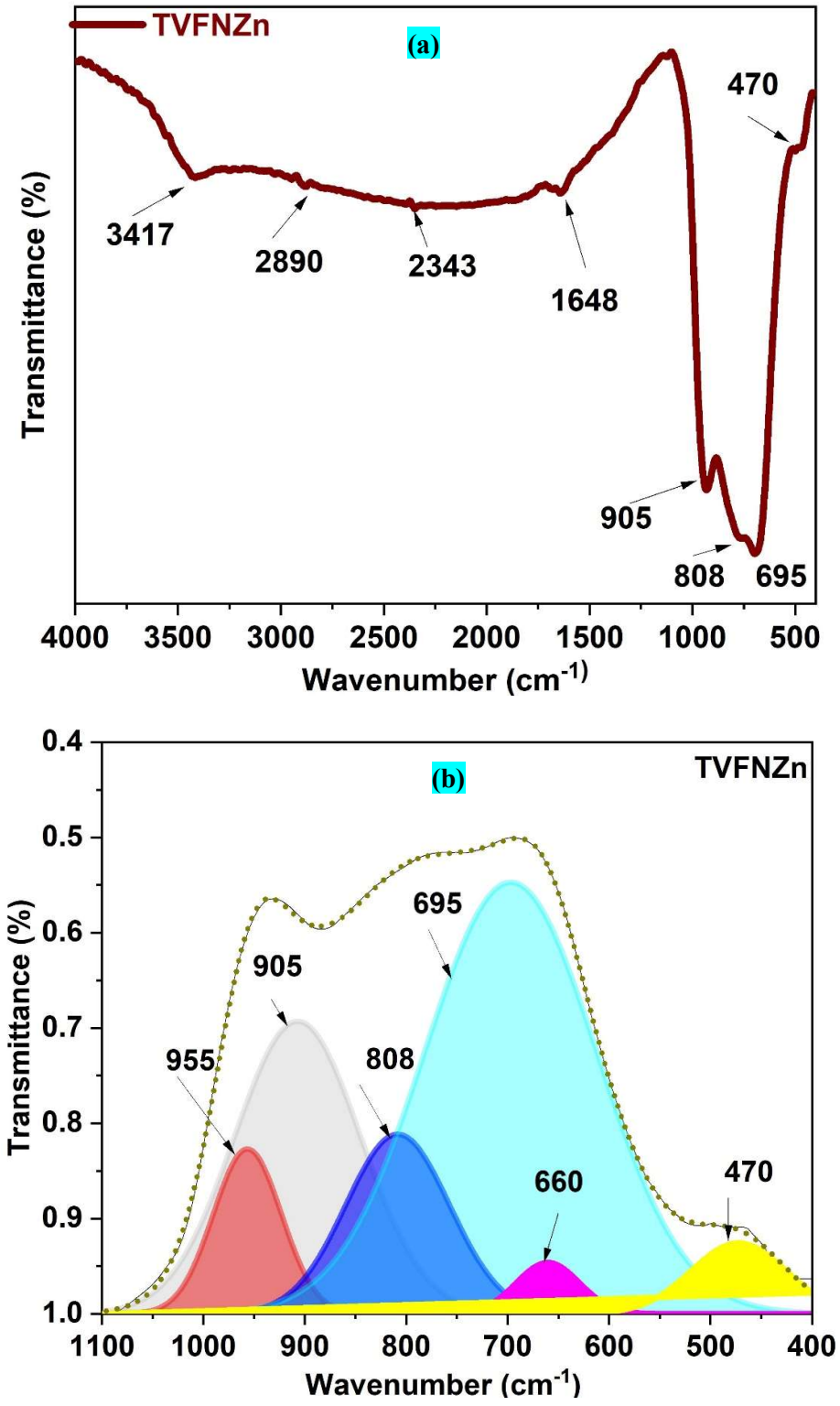

Fig. 1. (a) FT-IR spectra of Zinc doped tellurite glasses (b) De-convolution of the spectra.

4.2 Micro Raman analysis

The micro Raman bands in TVFNZn glasses at locations 127, 290, 469, 672, 732, 872, and 935 cm^{-1} span the wavelength range of 0 to 1200 cm^{-1}, as shown in Fig. 2. After the spectra were deconvoluted, the overlapping bands were seen in the 500–1100 cm^{-1} region. The skeletal bend vibration (B3g mode) is shown by the greatest intensity peak at 127 cm^{-1} [29]. The peaks that are closest to Raman shifts, at 291 cm^{-1}, have the highest intensity. A Raman band at 469 cm^{-1} is produced by the symmetrical stretching vibration of the Te-O-Te chain. The anti-symmetrical stretching vibration of the Te-O bond is represented by the band at 672 cm^{-1} in the $[TeO_4]^{4-}$ bi-pyramid. Two Te^{4+} ions are joined by this connection to produce a bridge O^{2-} ion [30]. The Te-O bond, which connects one Te^{4+} ion with a non-bridging O^{2-} ion, is what causes the band at 732 cm^{-1}. Additionally, the presence of either V^{2+} or Fe^{2+} ions causes the $[TeO_3]^{2-}$ pyramid and/or twisted $[TeO_{3+1}]$ to demonstrate charge balancing. According to reference [31], the asymmetric and symmetric stretching vibrations of VO_3 groups in TVFNZn glass are represented by the 872 and 935 cm^{-1} bands. Likewise, the triply coordinated oxygen (CO) stretching modes (V_3–O) are linked to the peak at 935 cm^{-1}. The doubly CO (V_2–O) stretching and bending vibrational modes that are part of the B2g symmetry vibration are responsible for the band at 872 cm^{-1}. Furthermore, the stretching mode seen at 935 cm^{-1} was attributed to the V = O bond [32]. The vibrations of Fe2O3 are represented by the Raman bands seen at 290, 469, and 672 cm^{-1} [33, 34].

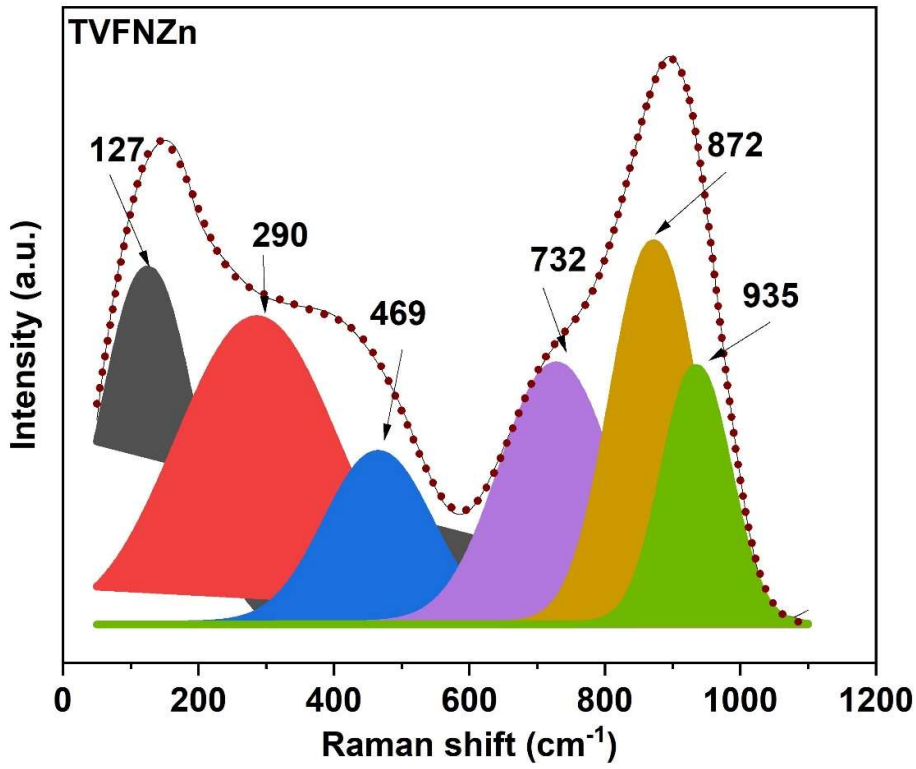

Fig. 2. Micro Raman spectra of Zinc doped tellurite glasses

4.3 ESR analysis

According to the Vandate ESR, there are magnetic resonance transitions between the fine structure-related triplet-state energy levels. The complexes show electron spin exchange interactions with a negligible anisotropic component contribution if our assumption that S′=1/2 is correct. As a result, one would anticipate seeing merely a change in line intensity when comparing spectra with exchange interaction present (for S′=1) and without (for S′=1/2) [35, 36].

TVFNZn glass was used for ESR experiments, and the resultant spectra are shown in Fig. 3. The inclusion of V_2O_5, Fe_2O_3, Na_2O, and ZnO revealed in Fig. 3(a) is probably the cause of the peak in the magnetic field (mT) vs. ESR intensity (a.u.) plot, which shows the presence of free radicals in the glass. Within the magnetic field range of 0 to 0.75 T, the signal's strength, which ranges from -1200 to 1500 a.u., is noticeably strong. The plot of *g*

value against ESR intensity is shown in Fig. 3(b). Te, V, and Fe ion multivalancy is represented by the curve intersecting the zero point at g values of 2.09 and 5.53. This finding implies that TVFNZn glasses contain free electrons, which enhance their magnetic characteristics.

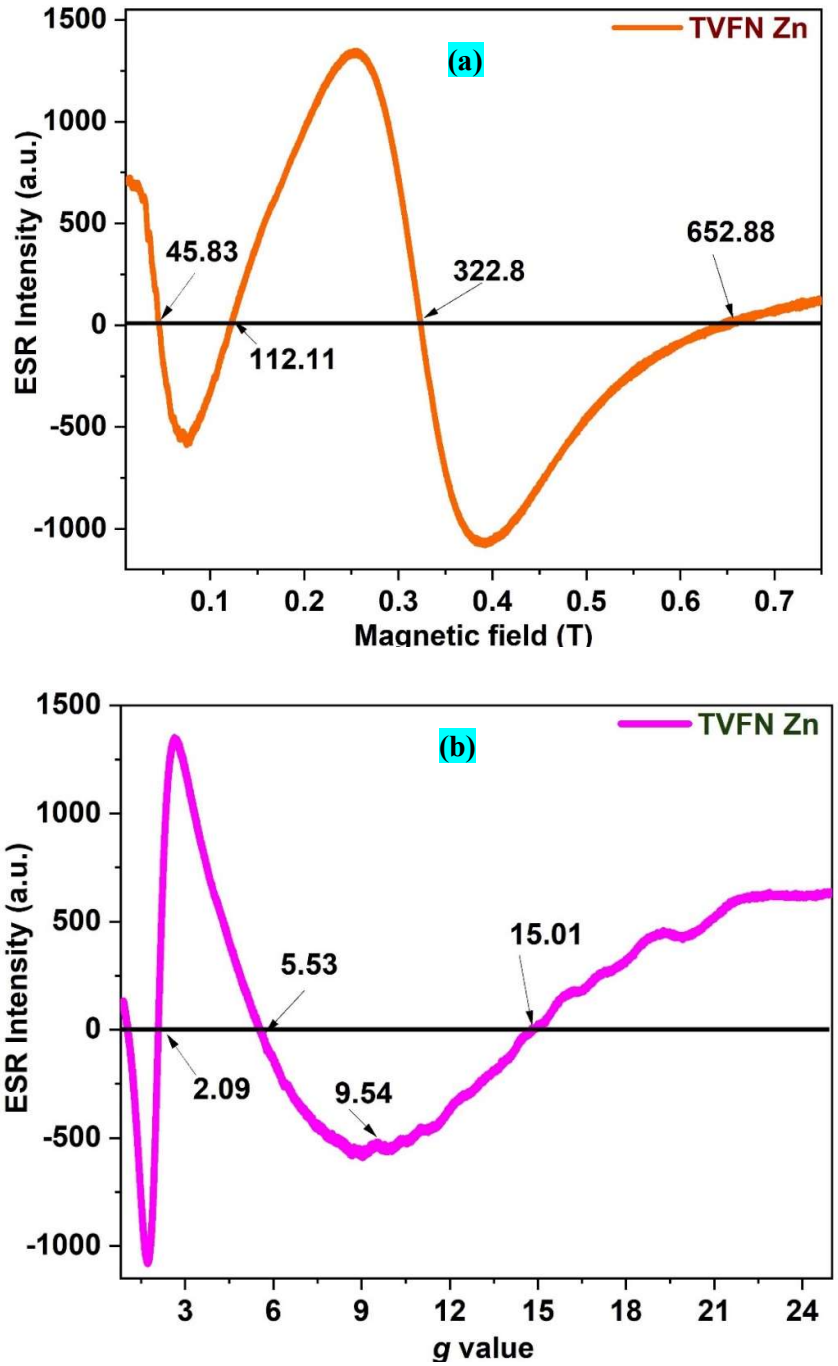

Fig. 3. ESR analysis of TVFNZn glasses (a) Magnetic field vs Intensity (b) g value vs intensity

4.4 VSM analysis

The vibrational sensing magnetometer (VSM), which uses the magnetic field vs. magnetisation (M-H) curve between the magnetic field range of -1.75 – 1.75 T, as seen in Fig. 4, provides a clear understanding of the materials' magnetic characteristics. The magnetisation (M) of the TVFNZn glasses rose as the applied magnetic field (H) increased, with saturation magnetisation as high as 0.2799 Am^2/Kg recorded. TVFNZn glass kept a magnetisation or remanence (M_r) of 22.883 x 10^{-3} Am^2/Kg when the field was switched off, and the magnetisation was lagging when the applied field was reduced after attaining the saturation point. It takes a negative magnetic field, or coersivity (H_c), of 2.2622 mT to remove the remanence from the TVFNZn glasses. The coersivity and remanance of TVFNZn glass indicate that the M-H curve showed tiny magnetic domains and a hysteresis loop-like magnetic material.

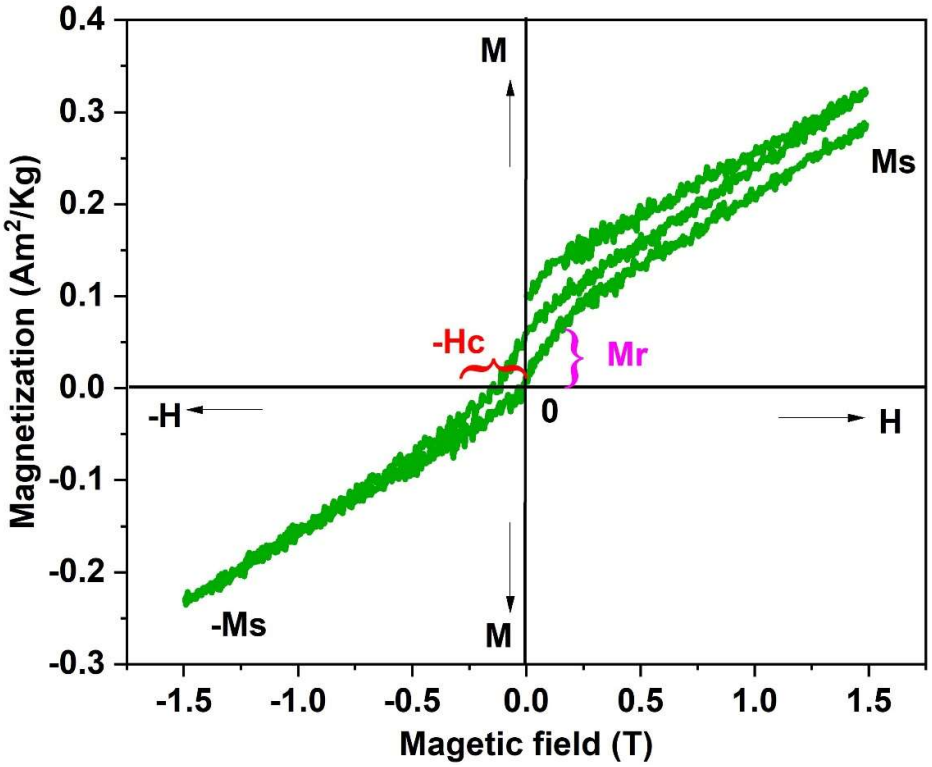

Fig. 4. Magnetic field vs Magnetization curve.

5.0 Optical properties

One useful method for examining electronic transitions in both crystalline and non-crystalline materials is optical absorption spectroscopy. Direct or indirect optical transitions take place between the valence and conduction bands across the optical band gap. Because glass-forming anions and cations (RE^{3+}) affect the conduction band and cause phonons to be absorbed or emitted, indirect transitions are often seen in vitreous materials. Figure 5 shows the optical absorption spectra of TVFNZn glasses utilising UV-visible-NIR spectroscopy in the 250–2500 nm range. For TVFNZn glasses, a small number of optical absorption bands were detected in the UV area at 275, 346, and 385 nm.TeO_2 is responsible for the absorption spectrum's UV band at 346 nm [37]. V_2O_5's absorption band is often seen between 200 and 300 nm [38]. For TVFNZn glasses, a noticeable band was seen in this area, perhaps as a result of the V_2O_5 material. Additionally, the 200–400 nm range is where the Fe_2O_3 band is seen [39].

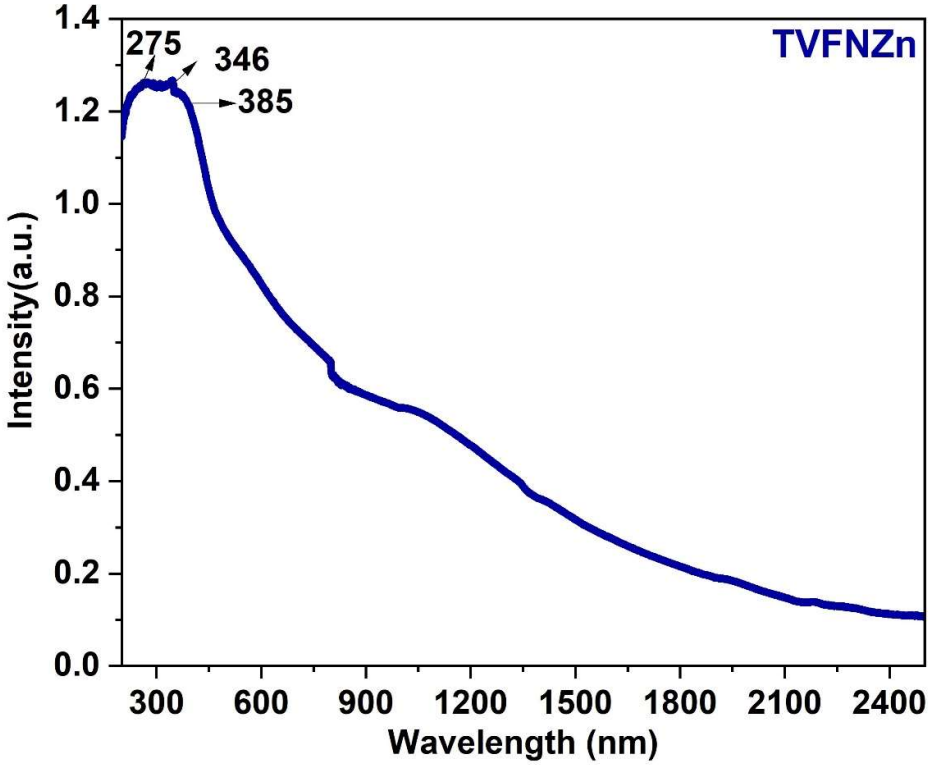

Fig. 5. Optical obsorption spectra of Zinc doped tellurite glasses.

5 Conclusion

Tellurite glasses modified with magnetic elements such as V_2O_5, Fe_2O_3, Na_2O, and ZnO (TVFNZn) were synthesized to investigate their structural, magnetic, and optical properties. FTIR analysis of the TVFNZn glasses revealed characteristic bands corresponding to the various metal oxides, while micro-Raman deconvolution identified additional unresolved bands. The magnetic moments in these glasses are attributed to the ionic states of vanadium, iron, and sodium, as determined through ESR analysis. The ESR spectra exhibited a g-factor of 2.09, indicating the presence of free electrons in the TVFNZn glasses. Magnetic behavior, characterized by hysteresis loops, was analyzed using a vibrating sample magnetometer, providing detailed magnetic parameters. The UV-Visible-NIR absorption spectrum of the glasses revealed distinct absorption bands. These findings suggest that TVFNZn glasses, with their pronounced paramagnetic properties, are promising candidates for applications in magneto-optical devices.

References

[1] G. Bendelli, S. Donati, E. Universita, and V. Abbiategrasso, Optical Isolators for Telecommunications: Review and Current Trends, Opt. Commun. 3, 373–380 (1992).

[2] L. Sun, S. Jiang, and J. R. Marciante, All-fiber optical magnetic-field sensor based on Faraday rotation in highly terbium-doped fiber, Opt. Express 18(6), 5407-5412 (2010).

[3] Douglas F. Franco, Roger G. Fernandes, Jorlandio F. Felix, Valmor R. Mastelaro, Hellmut Eckert, Conrado R.M. Afonso, Younes Messaddeq, Sandra H. Messaddeq, Steeve Morency, Marcelo Nalin, Fundamental studies of magneto-optical borogermanate glasses and derived optical fibers containing Tb3+, Journal of Materials Research and Technology 11 (2021) 312-327.

[4] David Vojna, Ondˇrej Slezák, Antonio Lucianetti and Tomáš Mocek, Verdet Constant of Magneto-Active Materials Developed for High-Power Faraday Devices, Appl. Sci. 2019, 9, 3160.

[5] G. Gao, A. Winterstein-Beckmann, O. Surzhenko, C. Dubs, J. Dellith, M.A. Schmidt, L. Wondraczek, Faraday rotation and photoluminescence in heavily Tb3+-doped GeO2-B2O3-Al2O3-Ga2O3 glasses for fiber-integrated magneto-optics, Sci. Rep. 5 (2015) 8942.

[6] Liviu Bolundut, Eugen Culea, Gheorghe Borodi, Razvan Stefan, Constantin Munteanu, Petru Pascut, Influence of Sm3þ:Ag codoping on structural and spectroscopic properties of lead tellurite glass ceramics, Ceramics International 41 (2015) 2931-2939.

[7] G Vijaya Prakash, D Narayana Rao, A.K. Bhatnagar, Linear optical properties of niobium-based tellurite glasses, Solid State Commun. 119 (2001) 39–44.

[8] P. Babu, Hyo Jin Seo, C.R. Kesavulu, Kyoung Hyuk Jang, C.K. Jayasankar, Thermal and optical properties of Er3þ-doped oxyfluorotellurite glasses, J. Lumin. 129 (2009) 444–448.

[9] N.V Ovcharenko, T.V Smirnova, High refractive index and magneto– optical glasses in the systems TeO2–WO3–Bi2O3 and TeO2–WO3–PbO, J. Non-Cryst. Solids 291 (2001) 121–126.

[10] A. Murali, R.P. Sreekanth Chakradhar, J. Lakshmana Rao, EPR studies of Gd3þ ions in lithium tetra boro-tellurite and lithium lead tetra borotellurite glasses, Physica B 364 (2005) 142–149.

[11] V. Himamaheswara Rao, P. Syam Prasad, P. Venkateswara Rao, Luís F. Santos, N. Veeraiah, Influence of Sb2O3 on tellurite based glasses for photonic applications, Journal of Alloys and Compounds 687 (2016) 898-905.

[12] G.V. Jagadeesha Gowda, C. Devaraja, B. Eraiah, A. Dahshan, S.N. Nazrin, Structural, thermal and spectroscopic studies of Europium trioxide doped lead boro-tellurite glasses, Journal of Alloys and Compounds 871 (2021) 159585.

[13] N.Chopa, A.ManningandG.Chadha, Electrical, optical and structural properties of amorphous V2O5-TeO2 blown films, J. Non-Cryst. Solids, 126, 194, 1990.

[14] Swapna, G. Upender, M. Prasad, Raman, FTIR, thermal and optical properties of TeO2 -Nb2O5-B2O3-V2O5 quaternary glass system, J. Taibah Univ. Sci. (2016).

[15] R. El-Mallawany, A. Abdel-Kader, M. El-Hawary, N. El-Khoshkhany, Volume and thermal studies for tellurite glasses, J Mater Sci (2010) 45:871–887.

[16] S.A. Salehizadeh, D. Souri, The glassy state of the amorphous V2O5– NiO–TeO2samples, Journal of Physics and Chemistry of Solids 72 (2011) 1381–1385.

[17] D. Souri, Crystallization kinetic of Sb–V2O5–TeO2glasses investigated by DSC and their elastic moduli and Poisson's ratio, Physica B 456 (2015) 185–190.

[18] Bezerra AG, Barison A, Oliveira VS, et al. The mechanism of cysteine detection in biological media by means of vanadium oxide nanoparticles. J Nanopart Res. 2012;14(9):1123.

[19] D. Rehder, Implications of Vanadium in Technical Applications and Pharmaceutical Issues, Inorganica Chimica Acta (2016).

[20] N. Elkhoshkhany, Ali Reda, Amira M. Embaby, Preparation and study of optical, Thermal, and Antibacterial Properties of vanadate–tellurite glass, Ceramics International 43, (17) (2017) 15635-15644.

[21] N.A. Zarifah, M. K. Halimah, M. Hashim, B. Z.Azmi, W. M. Daud, Magnetic Behaviour OF (Fe2O3)x (TeO2)1-x Glass System due to Iron Oxide, Chalcogenide Letters, 7 (9) (2010) 565 – 571.

[22] A. Dehelean, A. Popa, S .Rada, E. Culea, EPR and magnetic characterization of Fe2O3–TeO2 and CuO–TeO2 glasses obtained by melt quenching and sol–gel processes, Journal of Magnetism and Magnetic Materials 381 (2015) 131-137.

[23] Mahalakshmi S & Hema N & Vijaya P.P, In Vitro Biocompatibility and Antimicrobial activities of Zinc Oxide Nanoparticles (ZnO NPs) Prepared by Chemical and Green Synthetic Route— A Comparative Study, *BioNanoSci.* 10, 112–121 (2020).

[24] Imen Ben Elkamel, Nejeh Hamdaoui, Amine Mezni, Ridha Ajjel, Lotf Beji, Synthesis and characterization of Cu doped ZnO nanoparticles for stable and fast response UV photodetector at low noise current, Journal of Materials Science: Materials in Electronics, 30, 9444–9454 (2019).

[25] Shiliang Kang, Xiudi Xiao, Qiwen Pan, Dongdan Chen, Jianrong Qiu & Guoping Dong, Spectroscopic properties in Er^{3+}- doped germanotellurite glasses and glass ceramics for mid-infrared laser materials, Scientific Reports 7:43186 (2017).

[26] N. Elkhoshkhany, MA Khatab, Marwa A. Kabary, Thermal, FTIR and UV spectral studies on Tellurite Glasses doped with Cerium Oxide, Ceramics International 44 (3) (2018) 2789-2796.

[27] Joseph Raj Xavier, High protection performance of vanadium pentoxide-embedded polyfuran/epoxy coatings on mild steel, Polym. Bull. 78, 5713–5739 (2021).

[28] D.A. Magdas, O. Cozar, V. Chis, I. Ardelean, N. Vedeanu, The structural dual role of Fe2O3 in some lead-phosphate glasses, Vibrational Spectroscopy 48 (2008) 251–254.

[29] D. Surya Bhaskaram, Rajesh Cheruku, G. Govindaraj, Reduced graphene oxide wrapped V2O5 nanoparticles: green synthesis and electrical properties, J Mater Sci: Mater Electron, 27(2016)10855–10863.

[30] Gul Rahman, Oh-Shim Joo, Electrodeposited nanostructured a-Fe_2O_3 thin films for solar water splitting: Influence of Pt doping on photoelectrochemical performance, Materials Chemistry and Physics 140 (2013) 316-322.

[31] Puneet Kaur and Atul Khanna, Structural, electrical and luminescence properties of $M_2V_2O_7$ (M = Mg, Ca, Sr, Ba, Zn), Materials in Electronics 32 (2021) 21813–21823.

[32] Zili Wu, Adam J. Rondinone, Ilia N. Ivanov, and Steven H. Overbury, Structure of Vanadium Oxide Supported on Ceria by Multiwavelength Raman Spectroscopy, J. Phys. Chem. C 115 (2011) 25368–25378.

[33] Ningsi Zhang, Xin Wang, Jianyong Feng, Huiting Huang, Yongsheng Guo, Zhaosheng Li and Zhigang Zou, Paving the road toward the use of β-Fe_2O_3 in solar water splitting: Raman identification, phase transformation and strategies for phase stabilization, National Science Review 7: 1059–1067, (2020).

[34] Elizabeth C Pastrana, Victor Zamora, Dunwei Wang and Hugo Alarcón, Fabrication and characterization of α-Fe_2O_3/CuO heterostructure thin films via dip-coating technique for improved photoelectrochemical performance, Adv. Nat. Sci.: Nanosci. Nanotechnol. 10 (2019) 035012.

[35] Daniel Kivelson and Sai-Kwing Lee, ESR Studies and the Electronic Structure of Vanadyl Ion Complexes, The Journal of Chemical Physics 41 (7) (1964) 1896-1903.

[36] Taichi Sato, Takato Nakamura and Osamu Terao, Electron Spin Resonance Spectral Studies Of The Metal Complexes Formed In The Solvent Extraction Systems~Vanadyl Complexes With Long-Chain Alkyl Amine And Alkyl Ammonium Compound, J inore nucl Chem. 39. (1977) 401.404.

[37] J. Tauc, R. GrigorovicI, and A. Vancu, Optical Properties and Electronic Structure of Amorphous Germanium, phys. stat. sol. 15 (1966) 627-637.

[38] E. A. Davis a & N. F. Mott, Conduction in non-crystalline systems V. Conductivity, optical absorption and photoconductivity in amorphous semiconductors, The Philosophical Magazine: A Journal of Theoretical Experimental and Applied Physics, 22 (8) 179 (1970) 903-922.

[39] S. Hraiech, C. Bouzidi, M. Férid, Luminescence properties of Er^{3+}-doped phosphate Glasses, Physica B: Condensed Matter 522 (2017) 15-21.